Indian Journal of Information Sources and Services
ISSN: 2231-6094 (P), Vol.13, No.2, 2023, pp.46-52

DOI: https://doi.org/10.51983/ijiss-2023.13.2.3845

An Investigation of Fluid Flow Simulation in Bioprinting Inkjet Nozzles Based on Internet of Things

J. Priyanka[1], T. R. Poorani[2] and M. Ramya[3*]
[1]Department of Electronics and Communication Engineering, PSG College of Technology, Tamil Nadu, India
[2]Department of Biotechnology, Rajalakshmi Engineering College, Tamil Nadu, India
[3]Department of Biotechnology, Manipal Institute of Technology Bengaluru,
Manipal Academy of Higher Education, Karnataka, India
*E-mail: ramya.manohar@manipal.edu
(Received 6 November 2023; Revised 13 November 2023, Accepted 23 November 2023; Available online 25 November 2023)

***Abstract* - In the realm of 3D bioprinting, the ultimate objective is the creation of functional tissue constructs, achieved through precise control of inkjet performance and the ideal bioink composition. While the experimental standardization of these attributes can be time-consuming, their comprehension is facilitated through simulation analysis. In this paper, we use COMSOL Multiphysics to compare the rheological behaviour of three different bioprinting-friendly fluids: pure silk, silk mixed with PCL, and silk-PCL mixed with eggshell membrane. Our analysis focuses on the fluid flow dynamics in an air medium at various time intervals, specifically assessing the magnitude of velocity in each scenario. By considering both velocity and the uniformity of fluid dispersion throughout the inkjet process, we aim to identify the most advantageous fluid combination and optimal time interval for bioink applications. The transmission of this real-time data to a centralized Internet of Things (IoT) platform might facilitate the ability of researchers to remotely assess and visually represent the efficacy of various fluid combinations during the printing procedure.**
***Keywords:* Bioink, Silk, PCL, Egg Shell Membrane, Fluid Flow, COMSOL**

I. INTRODUCTION

Inkjet printers that create pictures on paper and operate according to the principle of the drop-on-demand contact approach [1] were first developed for this purpose. In recent years, inkjet printers have been utilized for a variety of additional applications that need the accurate deposition of microdroplets. This is possible because of the high resolution and acceptable speed that these printers exhibit. The field of life science is one application that makes use of such equipment for diagnosis, analysis, and the development of new drugs. Inkjets have also been utilized in 3D printers to synthesize tissues from cells by sequentially expelling droplets of bioink onto a substrate to replicate a computer-aided design (CAD) with printed tissue [1]. This process is known as inkjet tissue printing. One of the technologies that are connected to this is called bioprinting, and it uses bioink to create functional tissue constructions [2]. For these technologies to work properly, inkjet performance must be precisely controlled, and the bioink must have the ideal composition. However, further effort is required to develop standards for analyzing the performance of inkjet printers and the features of bioinks. The rate at which ink is injected into the nozzle of an inkjet printer is the factor that has the most impact on the printer's overall performance. This is because the rate at which ink is injected into the nozzle dictates the size of the droplets that are ejected.

Additionally, several other factors, such as the geometry of the inkjet and the fluid flow of the bioink, are amenable to suitable modification to produce droplets of varying sizes [3,4]. Even if the optimization of the fluid flow of bioink requires a very specific process, modeling and simulation work might be beneficial to comprehend these parameters more easily [5].

Natural polymers, such as collagen, alginate, hyaluronic acid, and gelatin, as well as synthetic polymers, such as polyethylene glycol (PEG), poly(lactic-co-glycolic) acid (PLGA), poly(-caprolactone) (PCL), and poly(L-lactic) acid (PLA), have been utilized in bioprinting even though each of these types of polymers has both positive and negative characteristics [6]. On the other hand, a formulation of bioink that is optimized may be achieved by combining natural and synthetic polymers to take use of the benefits offered by both types of materials [7,8].

PCL has been getting a lot of attention as a potential bioink material in recent years because it is biodegradable, biocompatible, and has a lot of penetrability. However, PCL does have a few drawbacks, the most significant of which are its very high crystallinity and slow degradation rate. The most straightforward approach to overcoming PCL's restrictions is to make composites using the material [9,10].

In this work, to research the comparative rheological performance of silk-based bioink, a COMSOL multiphysics simulation has been carried out to investigate the viscosity behaviour of silk fibroin and PCL bioink at various compositions and concentrations [11,12,13]. The results of this simulation show that the viscosity behaviour of silk fibroin and PCL bioink is quite similar. Studies of simulations have been carried out under these three situations. Silk was the fluid that was utilized in the beginning, then silk combined with PCL, and finally a mix of silk, PCL, and eggshell silk [14,15,16] was employed. It has been decided that air will serve as the medium. The Laminar Two-Phase Flow tool in COMSOL multiphysics was used to conduct a study of fluid flow with variable concentrations of fluid and velocities at which the analysis was completed.

The primary purpose of the effort is to produce the biomolecules that will be combined into bioink [17,18] utilizing silk fibroin, which will be derived from cocoons made of silk. The findings of this work may be applied to the characterization of newly produced bioink as well as the fluid flow analysis required for subsequent bioprinting of meniscal cavities in osteoblast cells. With the help of this work, an in-vitro investigation of the behaviour of osteoblast cells in the printed structure can also be calculated [19, 20, 21, 22]. This real-time data, when transmitted to a central IoT platform, enables researchers to remotely analyze and visualize the performance of different fluid combinations throughout the printing process [23].

II. DESIGN AND SIMULATION

The inkjet design exhibits a high degree of organization, featuring discrete areas labeled as follows: inlet, nozzle, outflow, and target, as illustrated in Figure 1(a). These regions also offer a comprehensive perspective of the inkjet's physical dimensions, which are presented in Figure 1(b). Notably, we have optimized the particulate size, a critical design parameter in bioprinting, in the development and dimensions of our inkjet [4].

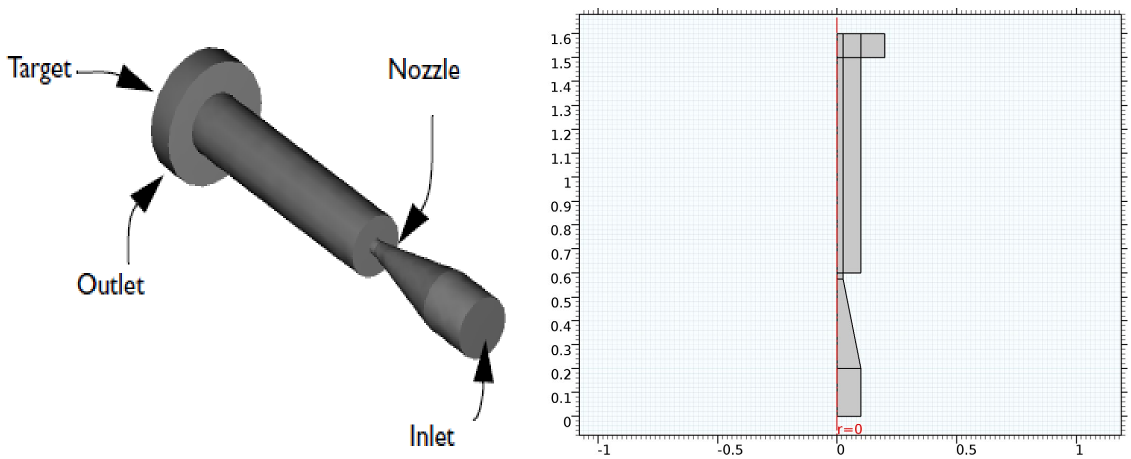

(a) (b)

Figure 1 Geometry of the inkjet (a) and (b) Dimensions of the inkjet

To aid comprehension of the inkjet's performance, a two-dimensional axisymmetric model that was intended to replicate real-world circumstances was constructed. The model illustrates the progression of ink from the inlet, through the ink supplementation phase that lasts for a duration of 10µs, filling the space between the inlet and the orifice. The surge of ink induces a regulated expulsion from the orifice, resulting in the separation of an ink particle that persists on its path until it arrives at the intended location [4]. At the entrance of the nozzle, a one-phase fluid flow is detected, which subsequently evolves into a two-phase flow as the ink passes through the air [10].

The simulation investigations required the assistance of laminar two-phase flow with two-dimensional axisymmetry. By applying the level-set physics principle, we investigated the motion of fluids and air with an emphasis on momentum and mass. The scope of the present inquiry included three distinct fluids, each represented by a different concentration and time interval: silk (5%), silk and PCL (5%–16%), and silk-PCL-eggshell (5%–16%) [4]. To obtain a thorough comprehension of the fluid dynamics, time intervals among 0s and $2e^{-4}$s [4] was examined.

The deliberate design of the mesh structure as a free triangular mesh guarantees the seamless identification of fluid flow. The following three conditions were identified as critical.

1. A bioink composed of silk fibroin (SF) and oxygen as the medium.
2. Silk fibroin in the medium of air with PCL as the bioink.
3. Eggshell membrane (ESM) and silk fibroin with PCL as the bioink and oxygen as the medium

The visual depictions of the initial air and ink distribution within the inkjet are presented in Figures 2(a) and (b), which offer insights into the characteristics of these fluids. In order to provide a comprehensive reference for our investigation, the material properties of air, silk fibroin, silk fibroin with PCL, and silk fibroin-eggshell membrane with PCL have been compiled in Table I.

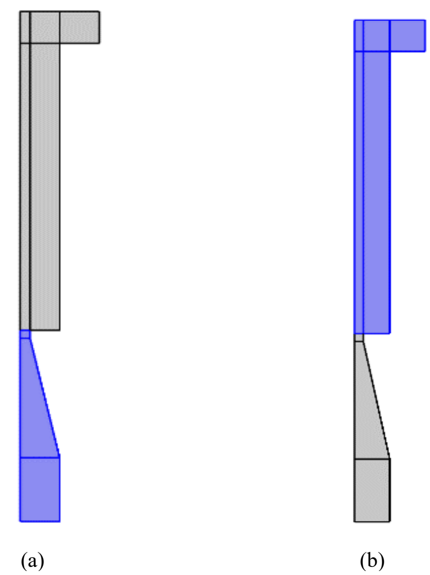

Fig. 2 Initial regions of (a) air and (b) ink distribution in the designed inkjet

TABLE I MATERIAL PROPERTY OF AIR AND SILK FIBROIN

Composition	Concentration	Name	Value	Unit
Air		Dynamic viscosity	$1.867x10^{-5}$	Pas
		Density	1.225	kg/m^3
Silk Fibroin Solution	SF- 5%	Dynamic viscosity	0.0099	Pas
		Density	1400	kg/m^3
Silk fibroin with PCL	SF- 5% PCL- 16%	Dynamic viscosity	0.12	Pas
		Density	1700	kg/m^3
Silk fibroin - egg shell membrane with PCL	SF- 5% PCL-16% ESM-1%	Dynamic viscosity	1.5	Pas
		Density	2000	kg/m^3

III. RESULTS AND DISCUSSION

The present investigation delves into the intricate world of velocity dynamics within inkjet bioprinting, with a specific focus on three key fluid conditions. The impact of varying time intervals on velocity magnitude, shedding light on how time affects fluid flow in this critical process was meticulously analyzed. In all scenarios, localized fluid distribution nearer to the nozzle, a consistent characteristic regardless of changes in time intervals was observed. It was found that even with varying time intervals, there was no substantial improvement in the distribution of silk throughout the inkjet.

For silk as the primary fluid, velocity decreased with increasing time intervals. Notably, even at zero-time intervals, velocity gradients due to air flowing through the nozzle were detected. Figure (3a) presents the initial velocity gradient at zero-time intervals, and subsequent figures (3b-f) illustrate the varying velocity magnitudes for different time intervals. The scenario changed when silk was combined with PCL, which exhibited a more uniform distribution with increasing time intervals until $8x10^{-5}$ s. However, at $1.6x10^{-4}$ s and $2x10^{-4}$ s time intervals, the fluid localized closer to the outlet region of the inkjet.

Comparatively, the $4x10^{-5}$ s time interval demonstrated the most uniform fluid distribution, thus representing the optimal choice for silk with PCL in the inkjet. In the third condition, employing a silk-egg shell membrane with PCL, a similar pattern emerged with a decrease in velocity magnitude as time intervals increased. Again, even at zero-time intervals, velocity gradients due to airflow was observed. Figure (5a) showcases the initial velocity gradient, and subsequent figures (5b-f) display the evolving velocity magnitudes for different time intervals.

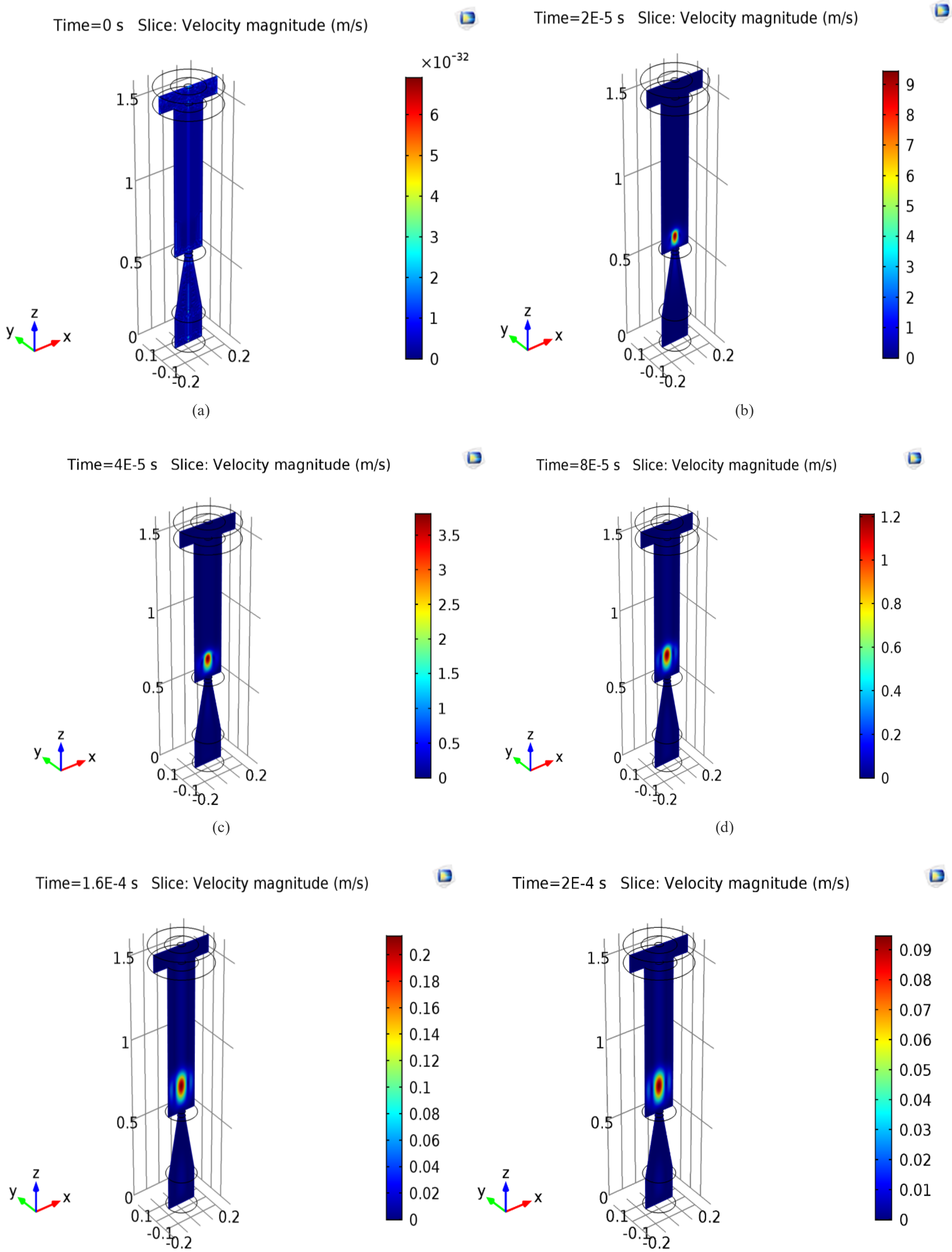

Fig. 3 (a-f) changes in velocity for different time intervals for silk in air medium

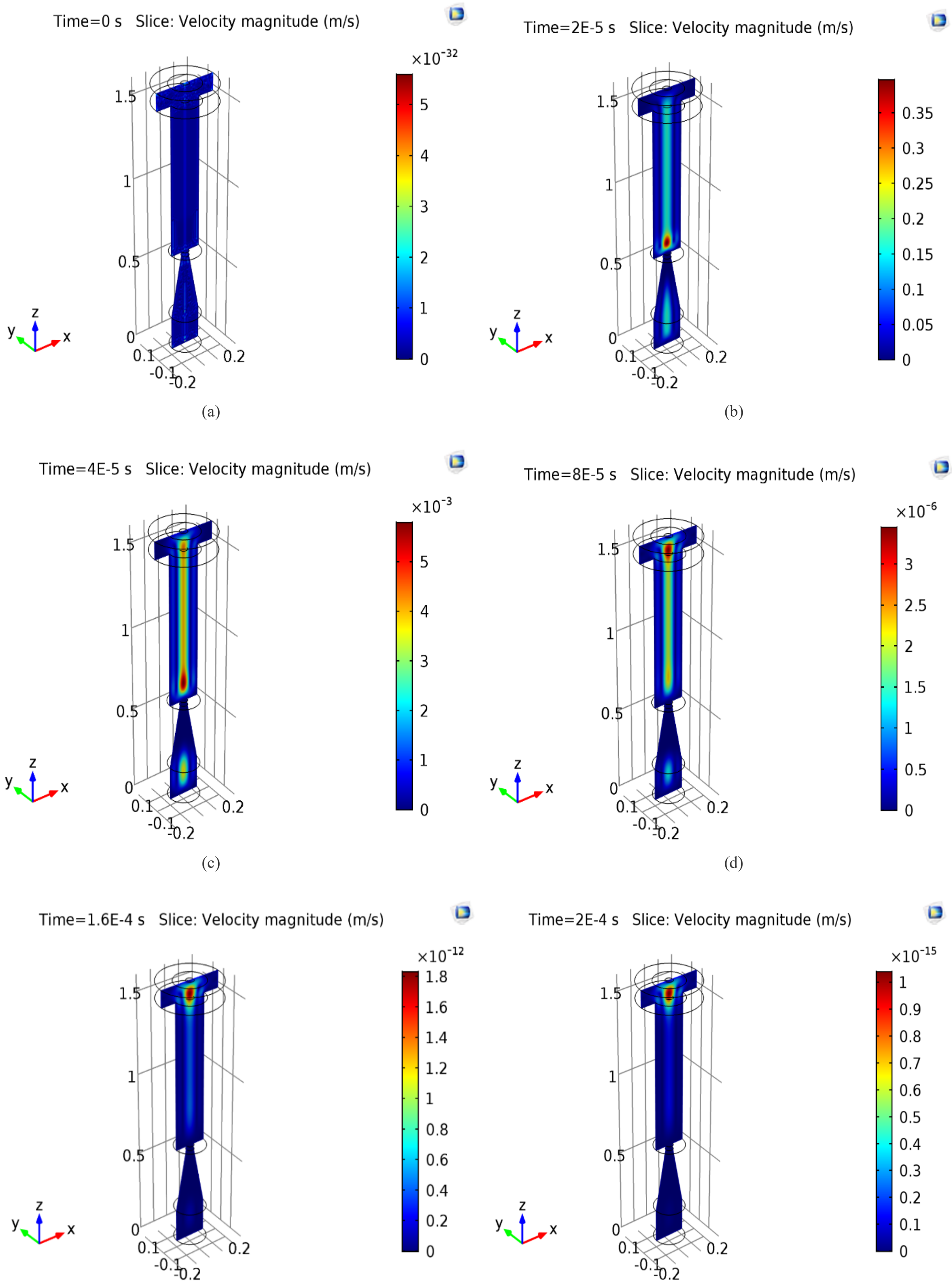

(a) (b) (c) (d) (e) (f)

Fig. 4 (a-f) Changes in velocity for different time intervals for silk with PCL in air medium

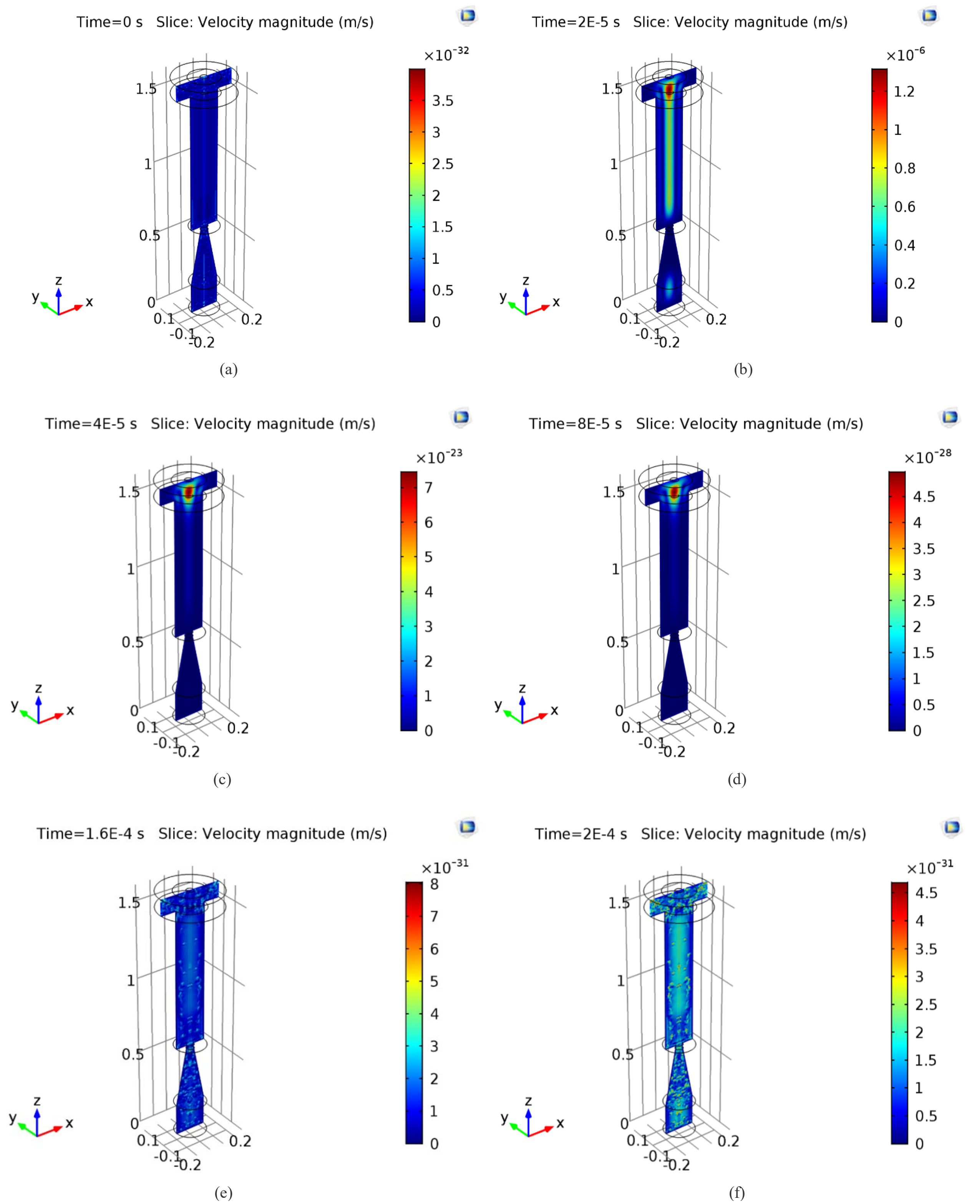

Fig. 5 (a-f) Changes in velocity for different time intervals for silk-egg shell membrane with PCL in air medium

In summary, this research highlights that fluid viscosity plays a pivotal role in the extrusion of fluid. More viscous fluids tend to remain within the nozzle. Silk and silk-egg shell membranes with PCL, due to their high viscosity, do not extrude readily. In contrast, silk combined with PCL displays uniform distribution and extrusion due to its more manageable viscosity. Consequently, the combination of silk with PCL emerges as the superior choice for bioink applications in this context.

IV. CONCLUSION

In the pursuit of enhancing bioprinting techniques, a comprehensive comparative analysis of the rheological performance of three different fluids, each with its potential suitability for bioprinting was conducted. Employing COMSOL Multiphysics, engaged in simulation studies under three distinct fluid conditions, employing air as the surrounding medium. The first fluid, silk, showcased a localized fluid distribution nearer to the nozzle across all observed time intervals. In contrast, the combination of silk and PCL revealed a notable improvement in fluid distribution uniformity, especially at the 4 x 10^{-5}s time interval. However, when the fluid composition encompassed silk, PCL, and eggshell membranes, the high viscosity resulted in a less uniform fluid distribution. So, our simulations showed that using silk combined with PCL at a time interval of 4 x 10^{-5}s was the best way to make sure that the fluid was spread out evenly in bioprinting applications. These results provide valuable insights for assessing the performance of bioinks in the realm of bioprinting. IoT technology would transform this research by providing continuous and data-driven insights, enabling more efficient and effective bioprinting processes.

REFERENCES

[1] Felix E. Montero, Rodrigo A. Rezende, Jorge V. L. da Silva & Marcos A. Sabino. (2019). Development of a Smart Bioink for Bioprinting Applications. *Frontiers of Mechanical Engineering, 5*, 56.

[2] Albertson, M. L, Dai, Y. B, Jensen, R. A, & Rouse, H. (1950). Diffusion of submerged jets. *Transactions of the American Society of Civil Engineers, 115*(1), 639-664.

[3] Allain, L. R., Stratis-Cullum, D. N., & Vo-Dinh, T., (2004). Investigation of microfabrication of biological sample arrays using piezoelectric and Bubble-jet printing technologies. *Analytica Chimica Acta, 518*(1), 77-85.

[4] Johan Gohl, KajsaMarkstedt, Andreas Mark, Karl Hakansson, Paul Gatenholm & Fredrik Edelvik. (2018). *Simulations of 3D bioprinting: predicting bioprintability of nanofibrillar inks, Biofabrication, 10*, 034105.

[5] Kan,g H. W., Yoo, J. J. & Atala, A., (2015). Bioprinted Scaffolds for Cartilage Tissue Engineering. *Methods in Molecular Biology, 1340*, 161-169.

[6] Cui, X., Boland, T., D'Lima, D. D. & Lotz, M. K., (2012). Thermal inkjet printing in tissue engineering and regenerative medicine. *Recent Patents on Drug Delivery and Formulations, 6*(2), 149-155.

[7] Lee, M. & Wu, B. M., (2012). Recent advances in 3D printing of tissue engineering scaffolds. *Methods in Molecular Biology, 868*, 257-267.

[8] Kundu, J., Shim, J. H., Jang, J., Kim, S. W. & Cho, D. W., (2013). An additive manufacturing based PCL-alginate-chondrocyte bioprinted scaffold for cartilage tissue engineering. *Journal of Tissue Engineering and Regenerative Medicine, 9*(11), 1286-1297.

[9] Shailendra Singh Shera, Nitin Kulhar Rathindra & Mohan Banik. (2019). Silk and silk fibroin-based biopolymeric composites and their biomedical applications. *Materials for Biomedical Engineering: Biopolymer Fibers, 11*, 339-374.

[10] Qiusheng Wang, Guocong Han, Shuqin Yan & Qiang Zhang. (2019). 3D Printing of Silk Fibroin for Biomedical Applications. *Materials, 12*, 504.

[11] Aneesia Varkey, Elakkiya Venugopal, Ponjanani Sugumaran, Gopinathan Janarthanan, Mamatha M. Pillai, Selvakumar Rajendran, Amitava Bhattacharyya. (2015). Impact of silk fibroin-based scaffold structures on human osteoblast MG63 cell attachment and proliferation. *International Journal of Nanomedicine, 10*, 43-51.

[12] Gloria, A. (2013). *Survey of Wild Silkmoth Populations in Three Ecological Zones and Evaluation of the Performance of Bobyx Mori.* University of Ghana Digital Collections.

[13] Zhaozhu Zheng, Jianbing Wu, Meng Liu, Heng Wang, Chunmei Li, María J Rodriguez, Gang Li, Xiaoqin Wang, David L Kaplan & Zhaozhu Zheng. (2017). 3D Bioprinting of Self-Standing Silk-Based Bioink. A*dvances in Healthcare Material,* 1701026.

[14] Paola Taddei, Valeria Chiono, Anna Anghileri, Giovanni Vozzi, Giuliano Freddi, Gianluca Ciardelli. (2013). Silk Fibroin/ Gelatin Blend Films Cross-linked with Enzymes for Biomedical Applications. *Macromolecular Bioscience, 13*(11), 1492-1510.

[15] María J. Rodriguez, Joseph Brown, Jodie Giordano, Samuel J. Lin, Fiorenzo G. Omenetto, David L. Kaplan. (2014). Silk based bio inks for soft tissue reconstruction using 3-dimensional (3D) printing with in vitro and in vivo assessments. *Biomaterials, 117,* 105-115.

[16] Yingxin Liu, Shengjie Ling, Suhang Wang, Xin Chen & Zhengzhong Shao. (2017). Thixotropic silk nanofibril-based hydrogel with extracellular matrix-like structure. *Biomaterials Science, 2*, 1338-1342.

[17] Amit Panwar & Lay Poh Tan. (2016). Current Status of Bioinks for Micro-Extrusion-Based 3D Bioprinting. *Molecules, 21*(6), 685.

[18] Fiona E. Freeman & Daniel J. Kelly. (2017). Tuning Alginate Bioink Stiffness and Composition for Controlled Growth Factor Delivery and to Spatially Direct MSC Fate within Bioprinted Tissues. *Scientific Reports, 7*, 17042.

[19] Lammel, A. S., Hu, X., Park, S. H., Kaplan, D. L., & Scheibel, T. R., (2010). Controlling silk fibroin particle features for drug delivery. *Biomaterials, 31*(16), 4583-4591.

[20] Das, S., Pati, F., Choi, Y. J., Rijal, G., Shim, J. H., Kim, S., & Ghosh, W. (2015). Bioprintable, cell-laden silk fibroin-gelatine hydrogel supporting multilineage differentiation of stem cells for fabrication of three-dimensional tissue constructs. *Acta Biomaterialia, 11,* 233-246.

[21] Gungor-Ozkerim, P. S., Inci, I., Zhang, Y. S., Khademhosseini, A., & Dokmeci, M. R., (2018). Bioinks for 3D bioprinting: an overview. *Biomaterials Science, 6*(5), 915-946.

[22] Derakhshanfar, S., Mbeleck, R., Xu, K., Zhang, X., Zhong, W. & Xing, M., (2018). 3D bioprinting for biomedical devices and tissue engineering: A review of recent trends and advances. *Bioactive Materials, 3*(2), 144-156.

[23] Buratti, C., Ström, E., Feltrin, L., Clavier L., Gardasevic, Blazek T., *et al.,* (2021). IoT protocols, architectures, and applications. *Inclusive Radio Communications for 5G and Beyond*, 187-220.